Potential Predictability of the Asian Summer Monsoon on Monthly and Seasonal Time Scales

R. S. Ajayamohan and B. N. Goswami
Centre for Atmospheric and Oceanic Sciences, Indian Institute of Science, Bangalore 560 012.

Email: goswamy@caos.iisc.ernet.in

Phone: 91-80-3600450

Fax: 91-80-3600865

To Appear in Meteorology and Atmospheric Physics

Corresponding author address:

B. N. Goswami, Centre for Atmospheric & Oceanic Sciences, Indian Institute of Science, Bangalore 560 012, India. E-mail: goswamy@caos.iisc.ernet.in

ABSTRACT

The potential predictability of the monthly and seasonal means during the Northern Hemisphere summer and winter is studied by estimating the signal-to-noise ratio. Based on 33 years of daily low level wind observations and 24 years of satellite observations of outgoing long wave radiation, the predictability of the Asian summer monsoon region is contrasted with that over other tropical regions. A method of separating the contributions from slowly varying boundary forcing and internal dynamics (e.g. intraseasonal oscillations) that determine the predictability of the monthly mean tropical climate is proposed. We show that the Indian monsoon climate is only marginally predictable in monthly time scales as the contribution of the boundary forcing in this region is relatively low and that of the internal dynamics is relatively large. It is shown that excluding the Indian monsoon region, the predictable region is larger and predictability is higher in the tropics during northern summer. Even though the boundary forced variance is large during northern winter, the predictable region is smaller as the internal variance is larger and covers a larger region during northern winter (due to stronger intraseasonal activity). Consistent with the estimates of predictability of monthly means, estimates of potential predictability on seasonal time scales also indicate that predictability of seasonal mean Indian monsoon is limited.

1. Introduction

The predictability of weather (or the instantaneous state of the atmosphere) is limited to about two weeks (Lorenz, 1982) due to inherent instability and nonlinearity of the system. The atmosphere, however, possesses significant low frequency variability. If the low frequency variations of the monthly and seasonal means were entirely governed by scale interactions of the higher frequency chaotic weather fluctuations, then the time averages will be no more predictable than the weather disturbances themselves. However, it appears that a large fraction of the low frequency variability in the tropics may be forced by slowly varying boundary conditions such as the sea surface temperature (SST), soil moisture, snow cover and sea-ice. Hence, the predictability of climate (e.g. space-time averages) is determined partly by chaotic internal processes and partly by slowly varying boundary forcings. This understanding that anomalous boundary conditions (ABC) may provide potential predictability has formed the scientific basis for deterministic climate predictions (Charney and Shukla, 1981; Shukla, 1981, 1998). Research during the past decade has shown that the climate in large part of tropics is largely determined by slowly varying SST forcing (Latif et al., 1998) where potential for making dynamical forecast several seasons in advance exists. However, during the same period, it has also been learnt that there are regions within the tropics, climate of which is not strongly governed by ABC. The Indian summer monsoon is such a system (Brankovic and Palmer, 1997; Goswami, 1998; Webster et al., 1998). The intraseasonal oscillations such as the eastward propagating Madden Julian Oscillations (MJOs) and the northward propagating monsoon Intraseasonal Oscillations (ISOs) with period in the range of 30 to 60 days are quite vigorous in the tropics. Both the MJOs as well as the monsoon ISOs are known to be driven by internal feedback between convection and dynamics. In addition to the scale interactions between weather disturbances, time-averaging of the chaotic ISOs can also contribute to the low frequency variability of monthly and seasonal means in the tropics. The nonlinear scale interaction associated with the weather disturbances in the

tropics is likely to be weak as they are less vigorous compared to their counterpart in the extratropics . Therefore, we envisage that most of the internal contribution to the low frequency variations in the tropics comes from time averaged residual of the ISOs.

Simulation of interannual variability of the Asian summer monsoon had generated lot of interest among the climate research community in the past two decades. Several modeling and observational studies have made serious attempts to estimate potential predictability of Asian summer monsoon. The fact that the simulation of interannual variability of monsoon rainfall differs from one model to another indicates the great sensitivity of this regional part of circulation on resolutions and physical parametrisations of the models (Gadgil and Sajani, 1998; Sperber and Palmer, 1996). While the prediction in other part of the tropics (e.g. Eq.Pacific and Sahel) does not seem to be sensitive to small changes in initial conditions, the simulation of seasonal mean monsoon seems to be rather sensitive to small changes in initial conditions (Brankovic and Palmer, 1997; Palmer and Anderson, 1994). This suggests that the mean monsoon circulation in the tropics may not be entirely forced by slowly varying SST boundary forcings but is also governed by internal dynamics to some extent. Here, we make quantitative estimates of contributions from boundary forcing and internal dynamics to the interannual variability to obtain an estimate of potential predictability of the Indian summer monsoon from observations.

The total low frequency variance of any variable in a given region (σ^2) could be written as super-position of variance due to external forcing (σ_e^2) and variance due to internal processes (σ_i^2). This ratio could be estimated using atmospheric general circulation models (AGCM) from a long integration with observed boundary condition and another long integration with fixed boundary condition (Goswami, 1998) or from an ensemble of long integrations of the AGCM with the same observed boundary conditions but the ensemble members differing only in the initial conditions (Harzallah and Sadourny, 1995; Rowell et al., 1995; Stern and Miyakoda, 1995). Estimates of potential predictability of

atmospheric interannual fluctuations can be deduced from the resulting ensemble dispersion. Kumar and Hoerling (1995) estimated the ratio between the external and internal variability for the extratropics using a large ensemble of long simulations by an AGCM. Zweirs and Kharin (1998) have examined the interannual variability and potential predictability of 850 hPa temperature, 500 hPa geopotential and 300 hPa stream function simulated by models that participated in the Atmospheric general circulation Model Inter-comparison Project (AMIP). They find that there is a wide variation in the ability of the AGCMs to simulate observed interannual variability, both total and weather noise induced. Krishnamurthy and Shukla (2001) used an ensemble of seven integrations with the Centre-for-Ocean-Land-Atmosphere Studies GCM with observed SST for 1979-98. They have noticed that model shows poor skill in simulating the interannual variability of monsoon over India. Calculation of variances of precipitation indices for model and observed data reveal that for the Indian land region the internal variability is quite close to SST forced variability. However, there is considerable consistency in the simulation of Indian monsoon precipitation within the ensemble members. Thus, the model simulations are not very sensitive to initial conditions but the model is unable to simulate the observed variability. Other models (e.g. Brankovic and Palmer, 1997) show that the spread among the ensembles in simulating the Indian summer monsoon rainfall is as large as the interannual variability itself. This indicates poor predictability of Indian monsoon rainfall. Note that the precipitation climatology of most of these models over the monsoon region is not realistic. Thus the current generation of AGCMs are unable to make an unambiguous estimate of the predictability of the Indian summer monsoon. Hence, there is a need to make a quantitative estimate of potential predictability of the Indian summer monsoon from observations. However, making unambiguous estimates of the 'internal' and 'external' components of variability from observations is rather difficult.

Primary objective of this study is to make a quantitative estimate of potential predictability of Asian monsoon climate on monthly and seasonal time scales. Many studies

in the past (Madden, 1976, 1981; Madden and Shea, 1978; Shea and Madden, 1990; Short and Cahalan, 1983; Shukla and Gutzler, 1983) estimated potential predictability of the extratropical climate from observations. Following the pioneering work of Charney and Shukla (1981), some others (e.g. Singh and Kriplani, 1986) also have attempted to estimate the potential predictability of the Indian summer monsoon. Zheng et al. (2000) have proposed a method to estimate potential predictability of seasonal means using monthly mean time series. Using this technique they have estimated the potential predictability of surface temperature, 500 hPa geopotential height and 300 hPa winds. The potential predictability tends to be high in the tropics and low in the extratropics as per their calculations. Singh and Kriplani (1986) estimated potential predictability of lower tropospheric monsoon circulation and rainfall over India for JJA season. Daily 700 hPa geopotential heights, mean sea level pressure and rainfall anomalies were used for the study. They found that potential predictability of seasonal lower tropospheric fields is low over the monsoon trough, but generally increases with decreasing latitude. For rainfall, potential predictability is about 50% over the major parts of the country. The reliability of the estimates of potential predictability in this study may be affected by insufficient data length. The method of removing the annual cycles which is important in this kind of analysis (Trenberth, 1984a) has not been outlined. Sontakke et al. (2001) have estimated potential predictability for long-range precipitation over the Indian subcontinent using precipitation data from 1901-1970. Their study indicate that the climate noise is small compared to climate signal over the Indian monsoon region. The F-ratio of JJAS precipitation ranges from 1.5 to 2.5, with high values on the west coast of India. This indicates certain amount of potential predictability of the seasonal mean. Due to differences in the methodology used and due to inhomogeneity of data used in different studies, it has been difficult to arrive at an universal conclusion regarding the quantitative measure of predictability over different geographical locations in general and the Indian monsoon region in particular.

With the availability of long term record of homogeneous atmospheric circulation data for over 40 years (e.g. from National Centre for Environmental Prediction/National Centre for Atmospheric Research Reanalysis), it is now worthwhile to re-examine the quantitative measure of potential predictability. While potential predictability over the global tropical belt will be estimated, the predictability of Asian monsoon region will be contrasted with that over the other tropical regions. In particular, we shall try to assess the contribution of the intraseasonal oscillations to the predictability. Here, we propose a method of separation of interannual variances of monthly means associated with the slowly varying externally forced component and from the internally determined component. The variances associated with the 'internal' and 'external' components are estimated. It is also demonstrated that the 'external' component separated by our method indeed represents the response of the tropical atmosphere to the slowly varying SST forcing. A measure of potential predictability is defined as the ratio between the 'total' (sum of 'external' and 'internal') and the 'internal' components. We use a method described by Trenberth (1984a, b) to estimate potential predictability of seasonal means. The data sets used for this study are described in section 2. The methodology used to estimate potential predictability of monthly means is presented in section 3. The role of intraseasonal oscillations in the monthly mean monsoon climate is also discussed in this section. Estimation of potential predictability of seasonal means is described in section 4. A summary of results is presented in section 5.

2. Data Used

The main data used in this study are the daily low level zonal winds (850 hPa) and 700 hPa geopotential height from NCEP/NCAR reanalysis (Kalnay et al., 1996) for 33 years (1965-1997) based on a state-of-the-art- global data assimilation system (including forecast model), that remains unchanged throughout the reanalysis period. As a result, the reanalysis overcomes the problems of non-stationary bias faced by earlier operational

analysis products. The forecast model used in the NCEP/NCAR reanalysis has a horizontal resolution of T62. Data is saved on a $2.5^\circ \times 2.5^\circ$ grid. One possible drawback of the reanalysis data is that a meteorological field may be influenced by systematic errors of the assimilation model in the data sparse region. Daily interpolated outgoing long wave radiation (OLR) data from the NOAA polar orbiting satellites for 20 years (1980 to 1999) were also used. This data set is taken from NOAA-CIRES Climate Diagnostics Center (CDC), Boulder, USA, from their website at http://www.cdc.noaa.gov/. Data gaps were filled with temporal and spatial interpolations; details of the interpolation technique can be found in Liebmann and Smith (1996). OLR data are available in $2.5^\circ \times 2.5^\circ$ latitude-longitude grid boxes.

3. Estimation of Potential Predictability of Monthly Means

3.1. Methodology

Here we outline a procedure to estimate potential predictability of monthly mean climate by describing a method to separate the 'external' and 'internal' components of monthly mean variability. Our methodology is based on the following premise. The anomalies associated with the synoptic and intraseasonal oscillations may be defined as the deviations from the annual cycle. The annual cycle at any place can be defined as the sum of the annual mean and first few harmonics of yearly data. In the present study, the annual cycle is defined as the sum of the annual mean and first three harmonics of daily data for each year. The annual cycle defined in this manner varies from year to year. An example of such interannual variations of the annual cycle of low level zonal winds at a point over the Indian Ocean is shown in Figure 1. It is clear that the annual cycle has significant year to year variations. We hypothesize that the interannual variations of the annual cycle are essentially forced by the slowly varying boundary forcing. The dominant slowly varying boundary forcing in the tropics is that associated with the El Nino and Southern Oscillation (ENSO) related SST variations. Since the time scale of

variations of the boundary forcing is much longer (3-4 years to decadal) than that of the annual cycle, it essentially modulates the annual cycle. Thus, the interannual variations introduced by the 'external' (slowly varying) forcing can be estimated from the monthly means constructed from the deviations of the individual annual cycles from the climatological mean annual cycle. Annual cycles of zonal winds at 850 hPa and geopotential height at 700 hPa for all years from 1965 to 1997 and those for OLR for all years from 1980 to 1999 are calculated. Climatological mean daily annual cycles of different fields are calculated from the daily annual cycles of individual years. Monthly 'external' anomalies are estimated as monthly means of deviations of individual annual cycles from the climatological annual cycle. If daily anomalies in a particular year is defined as the departure of daily observations from the annual cycle of that year, they represent the 'internal' contribution as the 'external' component represented by the interannual variation of the annual cycle is removed in this process. Thus, the monthly means of the daily anomalies constructed in this manner represent the 'internal' component. This definition implies that averaged over the whole year, the daily anomalies vanish. However, due to the intraseasonal oscillations, the monthly means are non-zero. Our definition of 'internal' monthly anomaly implies that it is contributed primarily by the intraseasonal oscillations and any 'climate noise' arising from higher frequency weather events is neglected. The 'internal' and 'external' monthly mean anomalies calculated in this manner are statistically independent as the temporal correlation between the two is nearly zero everywhere (figure not shown).

Let us define total monthly anomaly of any field (say, zonal wind) as sum of monthly anomalies associated with 'internal' and 'external' components.

$U_T(x, y, t) = U_E(x, y, t) + U_I(x, y, t)$

where subscripts E and I refer to the 'external' and the 'internal' components. Squaring both sides and summing over all months we can write the total variance to be given by sum of variances associated with the 'internal' and the 'external' components, namely

$\sigma_T^2 = \sigma_E^2 + \sigma_I^2$,

as the correlation between the 'internal' and the 'external' components is zero. The total interannual variance may be estimated in two ways. The traditional way of calculating it is to construct monthly mean data from the raw daily data. Then construct a climatological monthly mean annual cycle. Deviations of the monthly means from this climatological monthly mean annual cycle are the total monthly mean anomalies. The total interannual variance may be calculated from these total anomalies. Alternatively, daily anomalies can be constructed with respect to the daily climatological mean annual cycle. The monthly means obtained from these daily anomalies give us the total monthly mean anomalies.

Let U(m,n) represent any field for the n^{th} day of the m^{th}th year, where n= 1,2...365; m= 1,2...Y. The annual cycle ($U_a(m,n)$) is defined as the sum of the annual mean and first three harmonics of daily data for a year. Let p represent the days in a calendar month.

To find 'external' monthly anomalies:

Daily climatological mean of the annual cycle is defined as

$$U_{ca}(n) = \frac{1}{Y}\sum_{m=1}^{Y} U_a(m,n) \tag{1}$$

Daily 'external' anomaly is defined as

$$\tilde{U}(m,n) = U_a(m,n) - U_{ca}(n) \tag{2}$$

Monthly mean of 'external' anomalies

$$U_E(m,k)_{k=1..12} = \frac{1}{p}\sum_{n=1+p*(k-1)}^{p*k} \tilde{U}(m,n) \tag{3}$$

To find 'internal' monthly anomalies:

Daily 'internal' anomaly is defined as

$$\hat{U}(m,n) = U(m,n) - U_a(m,n) \tag{4}$$

Monthly mean of 'internal' anomalies

$$U_I(m,k)_{k=1..12} = \frac{1}{p} \sum_{n=1+p*(k-1)}^{p*k} \hat{U}(m,n) \tag{5}$$

To find 'total' monthly anomalies:

Daily climatological mean is defined as

$$U_c(n) = \frac{1}{Y} \sum_{m=1}^{Y} U(m,n) \tag{6}$$

Daily 'total' anomaly is defined as

$$U_T(m,n) = U(m,n) - U_c(n) \tag{7}$$

Monthly mean of daily anomalies

$$U^{'}(m,k)_{k=1..12} = \frac{1}{p} \sum_{n=1+p*(k-1)}^{p*k} U_T(m,n) \tag{8}$$

To test our claim that the 'external' anomalies estimated by this method are essentially driven by slowly varying SST changes associated with the ENSO, we carried out a combined EOF analysis of the monthly mean 'external' anomalies of OLR and winds at 850hPa. We have chosen the period between 1979 to 1997 for this analysis. The dominant EOF explaining about 20 percent of the total variance is shown in Figure 2. The spatial patterns of both OLR and low level winds correspond well with the canonical patterns associated with ENSO (Rasmusson and Carpenter, 1982; Wallace et al., 1998).

The principal component for the dominant EOF, PC1 (normalized by its own temporal variance) is also shown in Figure 2 together with normalized Nino3 SST anomalies. The correlation coefficient between PC1 and Nino3 (160°W-90°W, 5°S-5°N) SST anomalies is 0.84 indicating a strong link between the variability represented by the 'external' component and the ENSO. The second EOF and corresponding time coefficients (PC2) are not shown. However, PC1 and PC2 are strongly correlated at a lag of about 6 months. This lag-correlation together with the spatial patterns of the 'external' component represent an eastward propagation of the anomalies, again characteristic of the ENSO anomalies. Therefore, the 'external' component separated here clearly represents the response of the atmosphere to the slowly varying SST forcing associated with the ENSO. Actual anomalies of low level winds and OLR along the equator associated with the slow external forcing are shown in Figure 3. The magnitude of the anomalies during the warm and cold events are similar to those known to be associated with typical warm or cold phases of ENSO (Rasmusson and Carpenter, 1982) and the eastward propagation is also clearly seen.

3.2. Estimation of 'Internal' and 'External' Interannual Variances

The total variance of monthly means as well as the 'internal' and 'external' components of the variance of zonal winds at 850hPa (U_{850}) are calculated as described in the previous section based on daily data for 33 years (1965-1997). The three variances are shown in Figure 4. Similarly, the three variances for OLR are calculated based on available 20 years of daily data (1980-1999; figure not shown). To start with, we note that the sum of the 'external' and 'internal' variances almost exactly equals the total variances in all geographical locations in the tropics for both the fields. Secondly, it is clear from Figure 4(b) that the geographical distribution of the 'external' variances of low level zonal winds has the canonical pattern of the individual fields associated with the ENSO (Philander, 1990; Rasmusson and Wallace, 1983; Wallace et al., 1998). The

'external' variance of U_{850} has a major maximum centered around the dateline and a secondary maximum in the eastern equatorial Indian Ocean. Both the regions are known to be associated with large zonal wind anomalies during peak ENSO phases. It is also noted that most of the appreciable 'external' variance of either OLR or U_{850} is confined between 10°N and 10°S, characteristic of the Walker response associated with the ENSO. On the other hand, the 'internal' variances of U_{850} have large amplitude (Figure 4(c)) in the 'monsoon' regions of the tropics, namely the Indian summer monsoon region, the South China Sea monsoon region and the Australian monsoon region. We note that the 'internal' variance is generally smaller than that of the 'external' variance in the tropical Pacific. However, it could be comparable to or even larger than the 'external' variance in the monsoon regions mentioned above.

3.3. Potential Predictability of Monthly Means

Ideally, the potential predictability of either monthly or seasonal means climate is determined as the ratio between 'signal' to 'noise', the signal being the predictable 'external' component while the 'noise' being the 'internal' unpredictable component. Since it is normally difficult to separate the 'external' component from the 'internal' component, usually potential predictability is defined as the ratio (F-ratio) between total variance (σ^2) and climate noise (σ_i^2). In finding the potential predictability of the monthly means, since, we have separated the 'external' and 'internal' components, we can write

$$F = \frac{\sigma^2}{\sigma_i^2} = \frac{\sigma_e^2}{\sigma_i^2} + 1.$$

Larger the value of this ratio compared to two, higher the predictability. The F-ratio of two also signifies that the signal-to-noise ratio (i.e F-1) is equal to one and that half of the observed interannual variability is potentially predictable. The monthly mean climate may be considered marginally predictable if 'F' is greater but of the order two. If 'F' is less than two, the climate would be unpredictable as the 'internal' variability

exercises a dominating influence on the total monthly variability. This ratio for zonal winds at 850hPa for Northern Hemisphere (NH) summer (JJA) months is shown in Figure 5(a), while for winter (DJF) months are shown in Figure 5(b). Figure 5 represents the geographical distribution of potential predictability for U_{850}. Potential predictability is high wherever the ENSO influence is large in the summer months (Figure 5(a)). These include equatorial Pacific between 10°S and 10°N, equatorial Atlantic and equatorial Indian Ocean east of 70°E. Parts of Africa also indicate high predictability as this region is also known to have strong influence of ENSO. It may be noted from Figure 5(a) and Figure 5(b) that during the NH summer, not only the peak values of the 'F' are higher than those during northern winter, the area covered by 'F' greater than two is much larger during NH summer compared to that in NH winter. Thus, during NH winter the monthly mean predictability not only decreases compared to that in NH summer, the predictable region also shrinks. Over the Indian monsoon region 'F' ratio ranges between 2 and 3 during NH winter and goes even beyond 2 during NH summer.

The qualitative difference in the predictability regimes during NH summer compared to NH winter is probably not very surprising if we take into account the seasonality of the 'external' and the 'internal' variances. As the 'external' component of the variance arises from a slowly varying signal (with time scales longer than a year), we do not expect much seasonality in the 'external' variance. This is shown in Figure 6 for zonal winds at 850hPa. Except that the maximum variance occurs in the western Pacific during NH summer compared to central Pacific during winter, the general pattern of 'external' variance is similar in the equatorial wave-guide during both the seasons. The major difference between the 'external' variance between the two seasons occur in the central Pacific subtropics. This is due to the ENSO induced off equatorial response being much stronger during the NH winter than in the NH summer. However, the 'internal' variance has a pronounced seasonality (Figure 7). Barring Indian monsoon region and a small region in the American monsoon region, the internal variability is very week throughout

the equatorial wave-guide during NH summer. This explains the larger magnitude and extension of 'F' during NH summer (Figure 5(a)). On the other hand, the 'internal' variance during NH winter are quite strong from Indian Ocean to central Pacific, the maxima being over the Australian monsoon region and the South Pacific Convergence Zone (SPCZ). The larger 'internal' variability during NH winter is consistent with the fact the ISO activity in tropics is strong during boreal winter and spring and weak during boreal summer except over the Indian monsoon region (Madden and Julian, 1994; Wang and Rui, 1990). Even though the 'external' variance remains similar in magnitude and extent in winter compared to those in summer, the 'F' ratio becomes smaller and the predictable region shrinks to a smaller region in the far eastern Pacific due to vigorous 'internal' activity in Indian Ocean and central and western Pacific.

The 'F' ratio estimates for OLR for NH summer (JJA) months and NH winter (DJF) months are shown in Figure 8(a) and Figure 8(b) respectively. The potential predictability for convection (or precipitation) represented in Figure 8 shows that significant predictable region (e.g.'F' ≥ 2) for convection (or precipitation) is smaller than that for circulation. This region is mainly confined to the central and eastern equatorial Pacific coincident with the core predictable region of ENSO influence. The geographical distribution of potential predictability for OLR for NH winter months is shown in Figure 8(b). The predictable region gets confined to central and east equatorial Pacific. The noteworthy feature is that over the Indian monsoon region, 'F' ratios are less than two for convection. This indicates that the internal variability in the Indian monsoon region is even stronger than the potentially predictable 'external' component seriously limiting the predictability of the Indian summer monsoon.

The estimates of 'F' ratios for geopotential height at 700 hPa (Z_{700}) for NH summer (JJA) and NH winter (DJF) months are shown in Figure 9(a) and Figure 9(b) respectively. In contrast to the other fields discussed earlier such as U_{850} and OLR, the geopotential field at 700 hPa does not show a major maximum only over the central

equatorial Pacific. The whole tropical belt (10°S to 10°N) shows high values of potential predictability during summer (Figure 9(a)) as well as in winter (Figure 9(b)) months. The 'F' ratio generally decreases away from the equator. During the summer months, southern India shows high potential predictability while in the northern India and over the monsoon trough 'F' ratio ranges between 4 and 6. In the winter months also, 'F' ratios are high in the tropical belt. Both in summer and winter months 'F' ratio becomes less between 20°and 30°latitudes.

Since the geographical distribution of potential predictability of geopotential height is different from the other fields like zonal winds and convection, it might be interesting to look into the external and internal variances separately. In order to highlight the variance of the geopotential height in the tropics, the variances shown in Figure 10 and Figure 11 is restricted between 20°S and 20°N. This is because the variances of geopotential height in the extratropics tend to be several times larger than those in the tropics. The external variance of geopotential height is shown in Figure 10 for JJA and DJF months. The variance associated with the external component is quite high up to 120°E though some parts of Africa show lower variance. East equatorial Pacific also shows appreciable variance. For the winter months also, the variance up to 120°E is high. Over the Pacific, the peak shifts towards central Pacific. The spatial pattern of external variance of Z_{700} appears to have a wave number two structure. This is associated with the externally forced interannual variations of divergent Walker circulation. The geographical distribution of the variance of the geopotential height associated with the internal component for the summer and winter months is shown in Figure 11. In the summer months, internal variance is low in the entire tropical belt. While for the winter months internal variance values are nearly two times as high as those in summer months. The seasonal variation of internal variance is consistent with the observation that the intraseasonal oscillations in the equatorial region are stronger in the boreal winter as compared to the boreal summer. Here too, the variance values are high towards the

midlatitudes (not shown in Figure 11). The high external variance and the low internal variance in the tropics explain the high potential predictability in the tropical belt for geopotential height (Figure 9).

3.4. Role of Intraseasonal Oscillations

What is responsible for the 'internal' variability of the monthly means in the tropics? The synoptic disturbances in the tropics are much less energetic than their extratropical counterpart. Therefore, nonlinear interaction amongst the tropical synoptic disturbances is unlikely to result in significant energy in the low frequency regime (e.g. monthly and seasonal means). Moreover due to their high frequency, the monthly mean residuals from them are expected to be small. Therefore, the internal variability that could influence tropical monthly means are the monsoon ISOs during NH summer and the MJO in the other parts of the tropics. To test correctness of this conjecture, we calculate 'internal' variance after removing the synoptic disturbances from the daily anomalies. For this purpose, a Butterworth low-pass filter that keeps all periods greater than 10 days was applied on the daily anomalies of all years after removing the annual cycle of each individual years. Monthly mean anomalies, describing the 'internal' component, are again calculated by averaging the filtered anomalies over calendar months. The 'internal' variance calculated from the monthly means of the filtered data has no contribution from the synoptic variations and is solely contributed by the ISOs. The 'internal' variance calculated in this manner for U_{850} is shown in Figure 12. A comparison of Figure 12 with Figure 4(c) reveals that removal of the contribution of the synoptic disturbances from the daily data had no effect on the 'internal' variance either in magnitude or in spatial distribution. This analysis establishes that the 'internal' variability of the monthly means is entirely governed by the tropical ISOs.

4. Potential Predictability of Seasonal means

In this section, we define climate by seasonal mean and examine potential predictability of seasonal mean climate. The 'climatic signal' may arise from influences truly external to the climate system or it may arise from slowly varying modes of the entire climate system. An example of the latter is the El Nino and Southern Oscillation. The day to day fluctuations or 'weather' could give rise to variation of the seasonal mean through scale interaction. In tropics, day to day fluctuations of weather is rather weak, but the intraseasonal oscillations are strong. Hence the climate noise is mainly contributed by the scale interaction between weather disturbances and the ISOs. Since a season is significantly long compared to the typical time scale of the ISOs (30-60 days), the 'climate noise' arising due to the ISOs cannot be estimated by simple statistical averaging (as we did in the case of monthly means) but may be estimated by some kind of low frequency extension of high frequency spectrum. The focus of this section is to find out whether there is significant difference between interannual variations of seasonal mean climatic states that can be distinguished from the climate noise.

Trenberth (1984a, b) described a method to estimate the 'climate noise' as the low frequency extension of the high frequency component. We follow this method (method A of Trenberth (1984a)) to find an estimate of potential predictability of seasonal mean in the tropics, for the Northern Hemisphere summer and winter seasons. The potential predictability is defined as the ratio between interannual variance of the seasonal means and the 'climate noise'. The potential predictability of NH summer and NH winter seasons for low level zonal winds, OLR and geopotential height have been estimated. This part of the our study is not quite new except that we make use of a long homogeneous data set and that we focus on the potential predictability of the Indian monsoon region.

Figure 13 shows the geographical distribution of potential predictability for low level zonal winds (850 hPa) in NH summer and NH winter seasons. In NH summer, regions where the ENSO influence is large shows high predictability. The potential predictability

is maximum in the western equatorial Pacific, and is having an eastward extension over the central and eastern Pacific and equatorial Atlantic. Parts of Africa and eastern equatorial Indian ocean also shows high potential predictability. In NH winter, the maximum shifts towards central equatorial Pacific, but the pattern remains more or less similar. It is noteworthy that the Indian monsoon region have potential predictability values of the order of 1.5 in both the seasons which means that the monsoon climate is marginally predictable in the summer season. The 'climate noise' associated with U_{850} is shown in Figure 14. In the summer months, Asian monsoon region shows significant 'internal' variance. In the winter, variance maxima shifts towards the southern equatorial Indian Ocean and the Australian monsoon region shows high 'internal' variance. This indicate that the interannual variability of the intraseasonal oscillations in the Indian monsoon region in the NH summer monsoon season and Australian monsoon region in the NH winter season is comparable to the predictable component, limiting the predictability of the Indian and Australian monsoons.

Figure 15 shows the potential predictability distribution of convection (OLR) over the tropics in NH summer and winter seasons. Predictable regions shrinks in the case of convection compared to the large scale flow. In the summer season, western and central equatorial Pacific shows high predictability. Some parts of Africa and equatorial Atlantic also come under predictable regions. In the winter season, regions which have predominant ENSO influence show high predictability. Seasonal mean climate in Indian monsoon region is marginally predictable in the winter, but the 'F' ratios are less than two in the summer season. The convection is even less predictable than low level winds during the summer monsoon season.

Figure 16 shows the potential predictability distribution of geopotential height at 700 hPa over the tropics in NH summer and winter seasons. The 'F' ratios in the equatorial wave-guide is quite high both in the summer and winter seasons. In the both the seasons south equatorial Indian Ocean shows maximum predictability, though the

'F' ratios are high in the winter. 'F' ratios are low as we move up from 10°latitude. Indian region shows 'F' ratios between 3 and 6 for geopotential height. Southern India shows slightly higher 'F' ratios. This is consistent with the earlier study done in the region for the 700 hPa geopotential height (Singh and Kriplani, 1986). The 'climate noise' associated with geopotential height is much less over the Indian monsoon region, compared to interannual variance in both the summer and winter months (figure not shown). This explains, the high predictability associated with the geopotential height over the Indian monsoon region.

5. Discussions and Conclusions

In the present study, we attempt to determine the part of monthly and seasonal mean climate variability governed by 'internal' dynamics and that governed by 'external' slowly varying forcing from long daily observations. Potential predictability of the climate (monthly and seasonal means) is defined as the ratio of the interannual variance of the monthly or seasonal means and the 'internal' unpredictable component. Three different fields (low level zonal winds (850hPa), OLR and geopotential height at 700 hPa) are used for this purpose. Daily U_{850} and Z_{700} are taken from NCEP/NCAR Reanalysis for a period of 33 years (1965-1997). Daily OLR for 20 years (1980-1999) are also used.

The monthly mean climate over the monsoon regions of the world appear to have limited predictability. The 'F' ratio is close to 2 over the Indian monsoon region during summer and ranges between 2 and 3 over other monsoon regions which is much smaller compared to those over other regions in the tropics. In many recent studies, the difficulty in simulating and predicting the Indian summer monsoon has been attributed to the role of the ISOs (Goswami, 1995, 1998; Webster et al., 1998). In Goswami (1998), it was shown that the strength of the GCM simulated ENSO response decreases as we reach the Indian Ocean and Indian monsoon region and the internal variability could compete with the externally forced variability in this region. The present analysis shows, from

observation that the internal variability in the Indian summer monsoon region is indeed comparable to the boundary forced variability. However the fact that the F-ratio ranges between 2 and 3 indicates that the external forced predictable signal is slightly larger than the noise in some regions. Therefore, while deterministic prediction of the monthly mean summer monsoon climate may prove to be difficult, there exists some hope of limited predictability coming from the boundary forcing.

The other important result is that except over the Asian summer monsoon region, the monthly mean climate during the boreal summer is more predictable over a much larger region in the tropics than during boreal winter. As it is well known that the SST signal associated with the ENSO tends to peak during NH winter, it appeared counter intuitive that predictability should be weaker during this season. However, we show that the weaker and limited predictability during boreal winter is due to stronger internal variability associated with stronger ISOs during winter while the amplitude of the boundary forced variability remains similar to those in boreal summer. Thus, the monthly mean tropical climate seems to be more predictable in NH summer compared to NH winter over much of the tropical belt except in the Indian summer monsoon region.

The predictability of the seasonal mean climate over the Indian monsoon also region appear to be marginal. The 'F' ratio which is a measure of potential predictability is of the order of 1.5. As in the case of monthly mean climate, the Asian monsoon region is the region of lowest potential predictability of the seasonal climate during boreal summer. Barring the Indian monsoon region, most of the regions in the equatorial wave guide seem to have high potential predictability. Equatorial Pacific is associated with higher predictability values. Not surprisingly, regions that come under the influence of ENSO have high predictability.

As may be expected, the geographical distribution of potential predictability of the monthly and seasonal mean climate bear similarity in all the fields. Comparison between Figure 5(a) and Figure 13(a) reveal that the core predictable regions of monthly mean

climate in the summer months and that of the seasonal mean climate in the summer season is the same for low level zonal winds. Equatorial Pacific, equatorial Atlantic, south equatorial Indian Ocean and the African region seem to be highly predictable in both the cases. Over the Indian monsoon region, 'F' ratios are of the order of two in the monthly mean climate, while the ratios of the order of 1.5 in the seasonal mean. If we compare Figure 5(b) and Figure 13(b), it is clear that 'F' ratios are much larger in the central equatorial Pacific for the seasonal mean winter climate compared to the monthly mean climate in the winter months. Some parts of Africa, equatorial Indian Ocean and equatorial Atlantic comes under predictable regions in both the cases. Over the Indian monsoon region, 'F' ratio is of the order of two in the monthly mean climate, while it is of the order of 1.5 in the seasonal mean winter climate for low level zonal winds. Thus, it appears that the seasonal mean summer monsoon may be more difficult to predict compared to the monthly means of monsoon during boreal summer.

It may be noted that, of the three fields used in this study, low level zonal winds at 850 hPa and OLR shows similar characteristics in both monthly and seasonal mean potential predictability. But the geographical distribution of potential predictability of geopotential height at 700 hPa shows high potential predictability over almost the whole tropical belt. Within the tropics, the Indian summer monsoon region does show relatively lower potential predictability during boreal summer compared to rest of the tropics (Figure 9(a) and Figure 16(a)). However, the geopotential height seem to be predictable even over the Indian monsoon region. The difference in the potential predictability of the geopotential height and the circulation and convection fields is not surprising as the geopotential field in the tropics is not as strongly coupled to circulation field as in the extratropics due to breakdown of geostrophy close to equator. In the tropics, the transient disturbances (that give rise to internal variability) are driven not by available potential energy associated with mean temperature gradient but by potential energy associated with convection. That is why predictability is poorest for convection (OLR) and increas-

ingly higher for low level and upper level winds. Therefore, it is incorrect to conclude that Indian monsoon is predictable by simply looking at the geopotential height field. One need to look at the circulation, convection and precipitation fields to arrive at the correct picture of predictability of the monsoon.

Acknowledgment. This work is partially supported by a grant from the Department of Science & Technology, Government of India. R. S. Ajaya Mohan is supported by a fellowship from the Council of Scientific and Industrial Research (CSIR), India.

REFERENCES

Brankovic C, Palmer TN (1997) Atmospheric seasonal predictability and estimates of ensemble size. Mon Wea Rev 125: 859–874

Charney JG, Shukla J (1981) Predictability of Monsoons. In: Monsoon Dynamics (eds. Lighthill J, Pearce RP), Cambridge: Cambridge University Press, pp. 99–108

Gadgil S, Sajani S (1998) Monsoon precipitation in the AMIP runs. Climate Dynamics 14: 659–689

Goswami BN (1995) A multiscale interaction model for the origin of the tropospheric QBO. J Climate 8: 524–534

Goswami BN (1998) Interannual variations of Indian summer monsoon in a GCM: External conditions versus internal feedbacks. J Climate 11: 501–522

Harzallah A, Sadourny R (1995) Internal versus SST-forced atmospheric variability simulated by an atmospheric general circulation model. J Climate 8: 474–495

Kalnay E, Kanamitsu M, Kistler R, Collins W, Deaven D, Gandin L, Iredell M, Saha S, White G, Woollen J, Zhu Y, Leetmaa A, Reynolds R, Chelliah M, Ebisuzaki W, Higgins W, Janowiak J, Mo KC, Ropelewski C, Wang J, Jenne R, Joseph D

(1996) The NCEP/NCAR 40-year reanalysis project. Bull Amer Meteorol Soc 77: 437–471

Krishnamurthy V, Shukla J (2001) Observed and model simulated interannual variability of the Indian monsoon. Mausam 52: 133–150

Kumar A, Hoerling MP (1995) Prospects and limitations of atmospheric GCM climate predictions. Bull Amer Meteorol Soc 76: 335–345

Latif M, Anderson D, Barnett TP, Cane M, Kleeman R, Leetma A, O'Brien JJ, Rosati A, Schneider EK (1998) A Review of predictability and prediction of ENSO. J Geophys Res 103(C7): 14,375–14,393

Liebmann B, Smith CA (1996) Description of a complete (interpolated) outgoing longwave radiation dataset. Bull Amer Meteorol Soc 77: 1275–1277

Lorenz EN (1982) Atmospheric predictability experiments with a large numerical model. Tellus 43: 505–513

Madden RA (1976) Estimates of natural variability of time averaged sea level pressure. Mon Wea Rev 104: 942–952

Madden RA (1981) A quantitative approach to long range prediction. J Geophys Res 86: 9817–9825

Madden RA, Julian PR (1994) Observations of the 40-50 day tropical oscillation: A Review. Mon Wea Rev 122: 813–837

Madden RA, Shea DJ (1978) Estimates of natural variability of time averaged temperature over the United States. Mon Wea Rev 106: 1695–1703

Palmer TN, Anderson D (1994) The prospect of seasonal forecasting. A review paper. Quart J Roy Meteorol Soc 120: 785–793

Philander SG (1990) Elnino, Lanina and the Southern Oscillation. New York: Academic Press, 293 pp.

Rasmusson EM, Carpenter TH (1982) Variations in the tropical sea surface temperature and surface wind fields associated with Southern Oscillation/El Nino. Mon Wea Rev 110: 354–384

Rasmusson EM, Wallace JM (1983) Meteorological aspects of the ElNino/Southern Oscillation. Science 222: 1195–1202

Rowell D, Folland CK, Maskell K, Ward MN (1995) Variability of summer rainfall over tropical North Africa (1906-1992): Observations and modeling. Quart J Roy Meteorol Soc 121: 669–704

Shea DJ, Madden RA (1990) Potential for long range prediction of monthly mean surface temperature over north America. J Climate 3: 1444–1451

Short DA, Cahalan RF (1983) Interannual variability and climate noise in satellite observed long-wave radiation. Mon Wea Rev 111: 572–577

Shukla J (1981) Dynamical predictability of monthly means. J Atmos Sci 38: 2547–2572

Shukla J (1998) Predictability in the midst of chaos: a scientific basis for climate forecasting. Science 282: 728–731

Shukla J, Gutzler DS (1983) Interannual variability and predictability of 500 mb geopotential heights over the northern hemisphere. Mon Wea Rev 111: 1273–1279

Singh SV, Kriplani RH (1986) Potential Predictability of lower-tropospheric monsoon circulation and rainfall over India. Mon Wea Rev 114: 758–763

Sontakke NA, Shea DJ, Madden RA, Katz RW (2001) Potential for long-range regional precipitation over India. Mausam 52: 47–56

Sperber KR, Palmer TN (1996) Interannual tropical rainfall variability in general circulation model simulations associated with Atmospheric Model Intercomparison Project. J Climate 9: 2727–2750

Stern W, Miyakoda K (1995) The feasibility of seasonal forecasts inferred from multiple GCM simulations. J Climate 8: 1071–1085

Trenberth KE (1984a) Some effects of finite sample size and persistence on meteorological statistics. Part I: Autocorrelations. Mon Wea Rev 112: 2359–2368

Trenberth KE (1984b) Some effects of finite sample size and persistence on meteorological statistics. Part II: Potential predictability. Mon Wea Rev 112: 2369–2379

Wallace JM, Rasmusson EM, Mitchell TP, Kousky VE, Sarachik ES, von Storch H (1998) On the structure and evolution of ENSO-related climate variability in the tropical Pacific. J Geophys Res 103(C7): 14,241–14,259

Wang B, Rui H (1990) Synoptic Climatology of Transient Tropical Intraseasonal Convection Anomalies: 1975-1985. Meteorol Atmos Phys 44: 43–61

Webster PJ, Magana VO, Palmer TN, Shuka J, Tomas RT, Yanai M, Yasunari T (1998) Monsoons: Processes, predictability and the prospects of prediction. J Geophys Res 103(C7): 14,451–14,510

Zheng X, Nakamura H, Renwick JA (2000) Potential predictability of seasonal means based on monthly time series of meteorological variables. J Climate 13: 2591–2604

Zweirs F, Kharin VV (1998) Intercomparison of interannual variability and predictability in : an AMIP diagnostic subproject. Climate Dynamics 14: 517–528

Printed October 12, 2002.

Figure Captions

FIG. 1. An illustration of variations of the annual cycle from year to year. The annual cycle of zonal winds (ms^{-1}) at 850hPa at a point (80°E, 5°N) are shown for 5 years.

FIG. 2. First combined EOF of mean monthly 'external' anomalies for the period January 1979 to December 1997 (228 months). (a) Zonal winds EOF at 850hPa, (b) OLR EOF and (c) PC1 (solid line) and Nino3 SST anomalies (dashed line). Both the time series are normalized by their own standard deviation. Units of the EOF's are arbitrary.

FIG. 3. Time-longitude section of mean monthly 'external' anomalies of zonal wind at 850hPa (ms^{-1}) and OLR (Wm^{-2}) averaged around equator (5°S-5°N). Positive contours are shaded. Contour interval for U_{850} is 2 units with minimum contour 1. Contour interval for OLR is 5 units with minimum contour 5.

FIG. 4. Monthly variance of zonal winds (m^2s^{-2}) at 850hPa based on 396 months for the period January 1965 to December 1997. (a) Total variance (b) 'external' variance and (c) 'internal' variance.

FIG. 5. Estimates of 'F' ratios for zonal winds at 850hPa (a) for all NH summer months (JJA) and (b) for all NH winter months (DJF) during the period 1965-1997.

FIG. 6. The 'external' variance of zonal winds at 850hPa (m^2s^{-2}) during (a) NH summer months (JJA) and (b) NH winter months (DJF).

FIG. 7. The 'internal' variance of zonal winds at 850hPa (m^2s^{-2}) during (a) NH summer months (JJA) and (b) NH winter months (DJF).

FIG. 8. Estimates of 'F' ratios for OLR (a) for all NH summer months (JJA) and (b) for all NH winter months (DJF) during the period 1980-1997.

FIG. 9. Estimates of 'F' ratios for geopotential height at 700 hPa (a) for all NH summer months (JJA) and (b) for all NH winter months (DJF) during the period 1965-1997.

FIG. 10. The 'external' variance of geopotential height at 700 hPa (gpm^2) during (a) NH summer months (JJA) and (b) NH winter months (DJF).

FIG. 11. The 'internal' variance of geopotential height at 700 hPa (gpm^2) during (a) NH summer months (JJA) and (b) NH winter months (DJF).

FIG. 12. The 'internal' variance of zonal winds at 850hPa (m^2s^{-2}) based on 396 months for the period January 1965 to December 1997 after removing the higher frequencies with period shorter than 10 days.

FIG. 13. Estimates of 'F' ratios for zonal winds at 850hPa for (a) NH summer season (JJA) (b) NH winter season (DJF).

FIG. 14. Estimates of 'climate noise' for zonal winds at 850hPa for (a) NH summer season (JJA) (b) NH winter season (DJF).

FIG. 15. Estimates of 'F' ratios for OLR for (a) NH summer season (JJA) (b) NH winter season (DJF).

FIG. 16. Estimates of 'F' ratios for geopotential height at 700hPa for (a) NH summer season (JJA) (b) NH winter season (DJF).

Figures

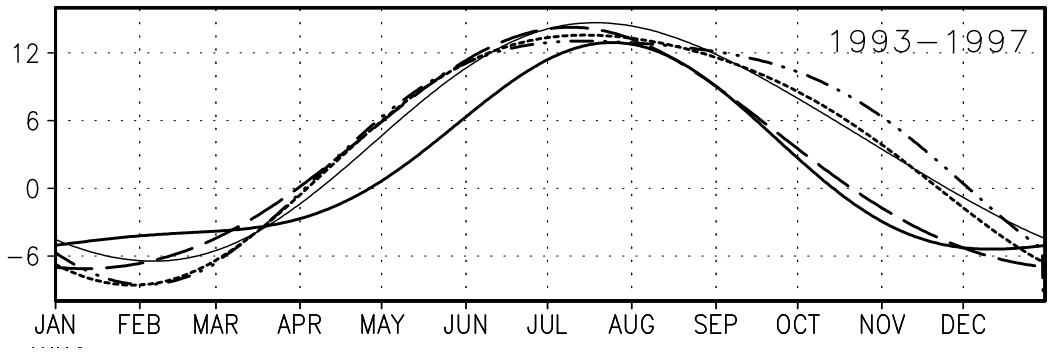

FIG. 1. An illustration of variations of the annual cycle from year to year. The annual cycle of zonal winds (ms^{-1}) at 850hPa at a point (80°E, 5°N) are shown for 5 years.

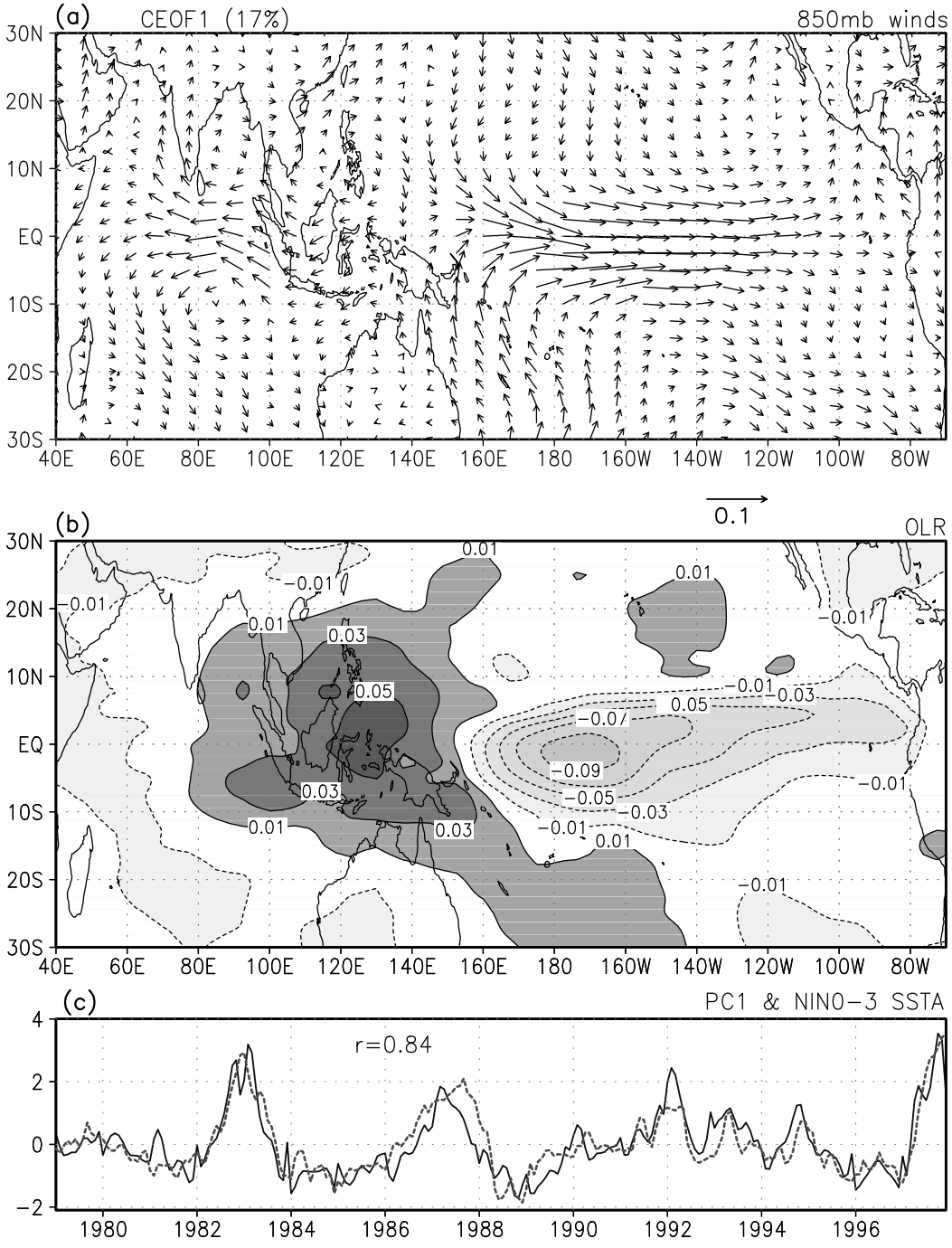

FIG. 2. First combined EOF of mean monthly 'external' anomalies for the period January 1979 to December 1997 (228 months). (a) Zonal winds EOF at 850hPa, (b) OLR EOF and (c) PC1 (solid line) and Nino3 SST anomalies (dashed line). Both the time series are normalized by their own standard deviation. Units of the EOF's are arbitrary.

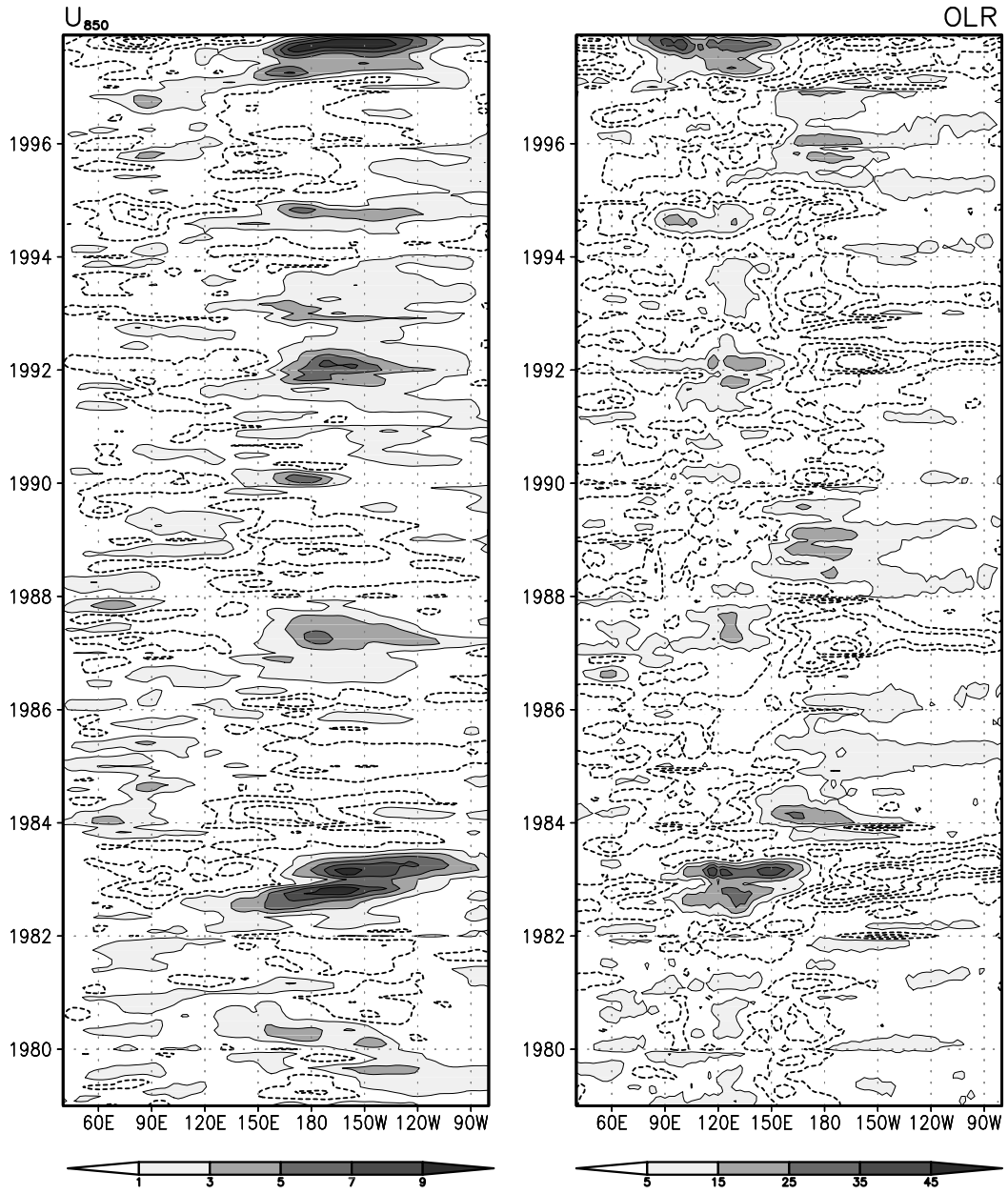

FIG. 3. Time-longitude section of mean monthly 'external' anomalies of zonal wind at 850hPa (ms^{-1}) and OLR (Wm^{-2}) averaged around equator (5°S-5°N). Positive contours are shaded. Contour interval for U_{850} is 2 units with minimum contour 1. Contour interval for OLR is 5 units with minimum contour 5.

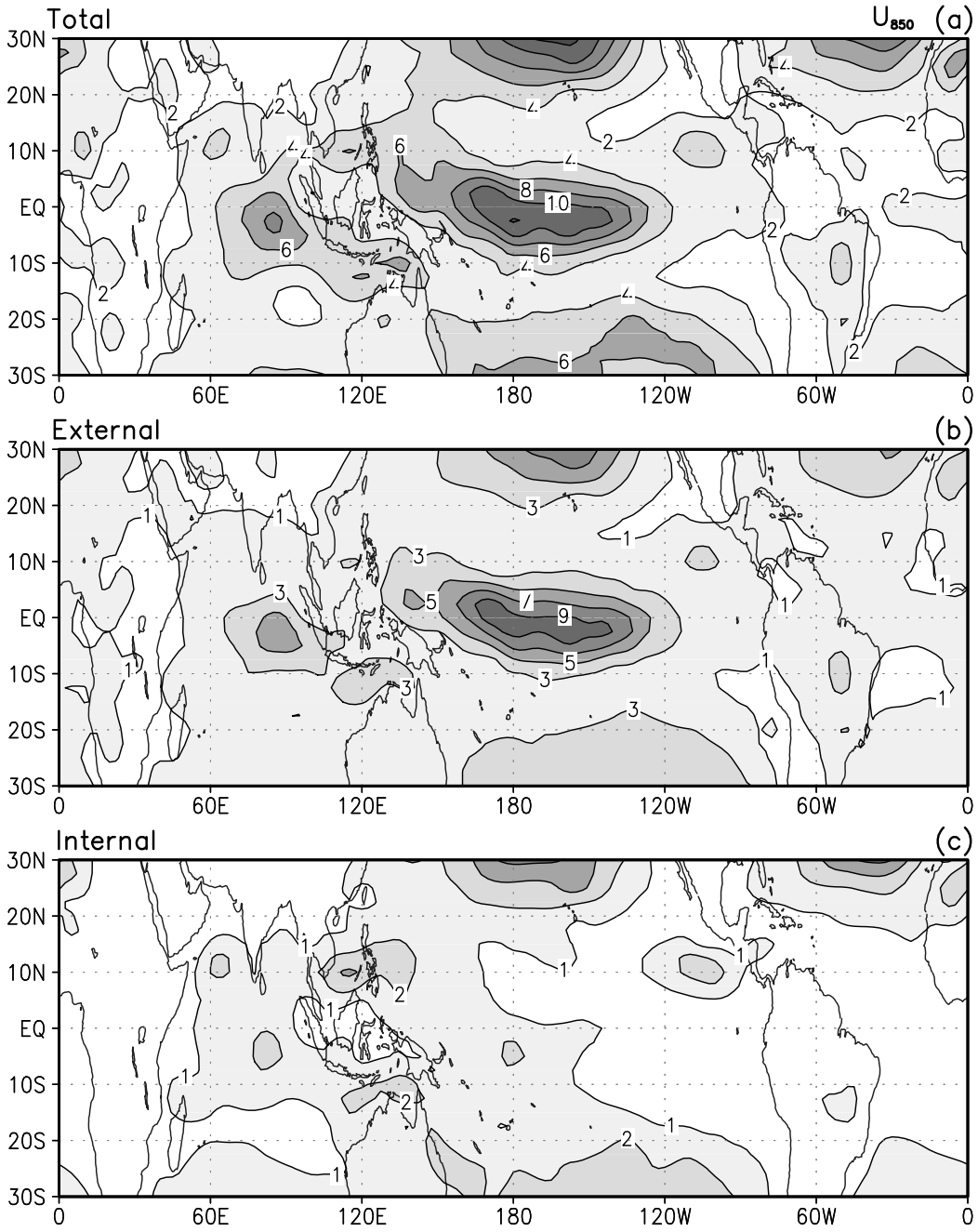

FIG. 4. Monthly variance of zonal winds (m^2s^{-2}) at 850hPa based on 396 months for the period January 1965 to December 1997. (a) Total variance (b) 'external' variance and (c) 'internal' variance.

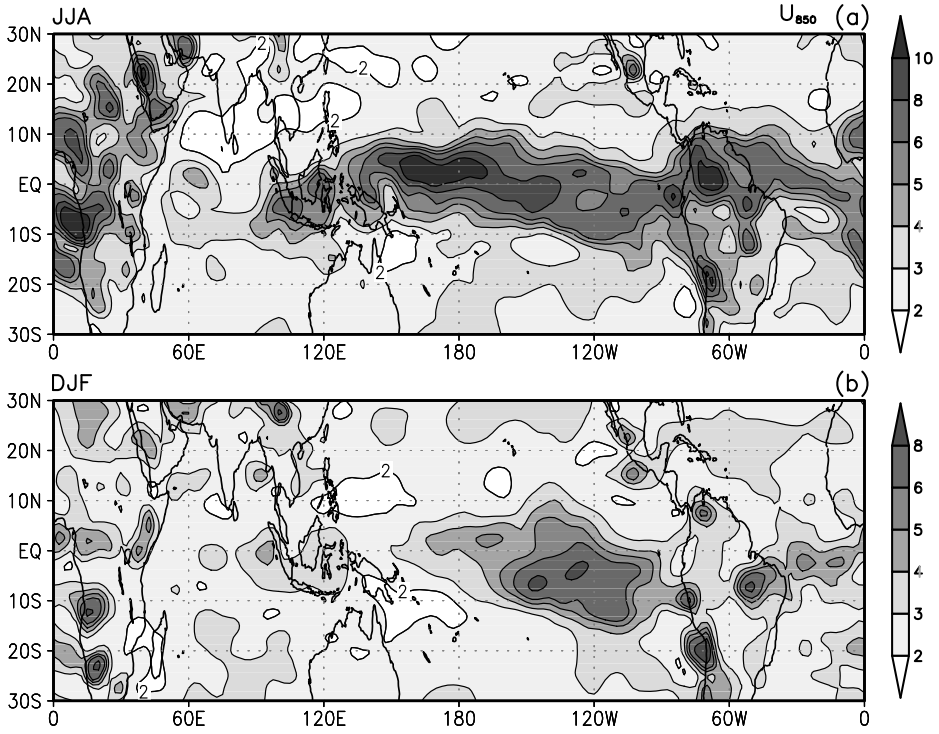

FIG. 5. Estimates of 'F' ratios for zonal winds at 850hPa (a) for all NH summer months (JJA) and (b) for all NH winter months (DJF) during the period 1965-1997.

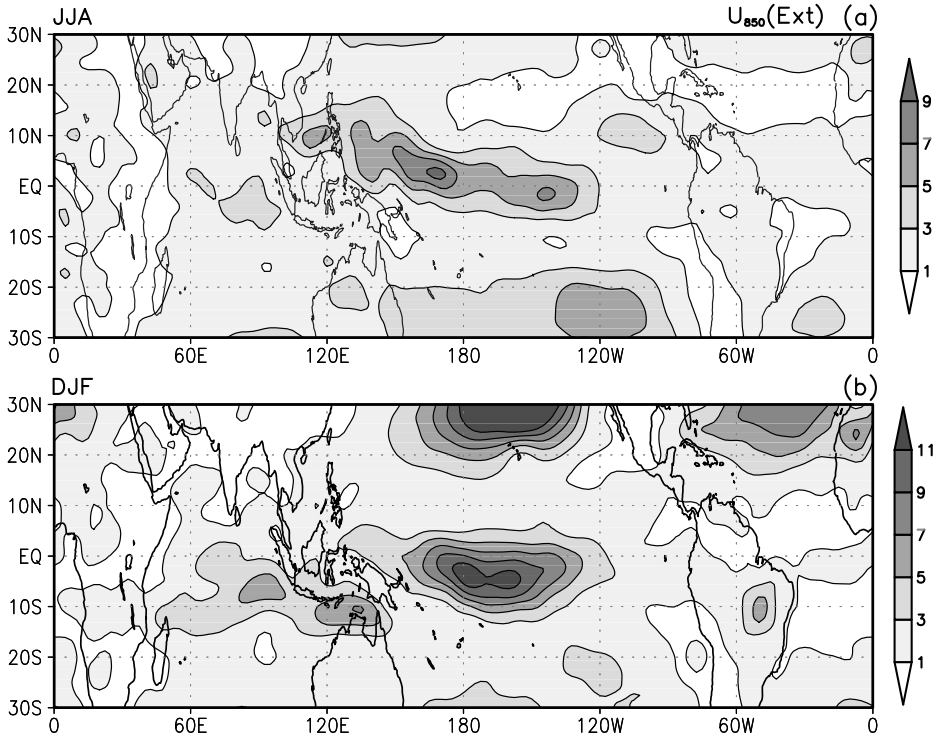

FIG. 6. The 'external' variance of zonal winds at 850hPa (m^2s^{-2}) during (a) NH summer months (JJA) and (b) NH winter months (DJF).

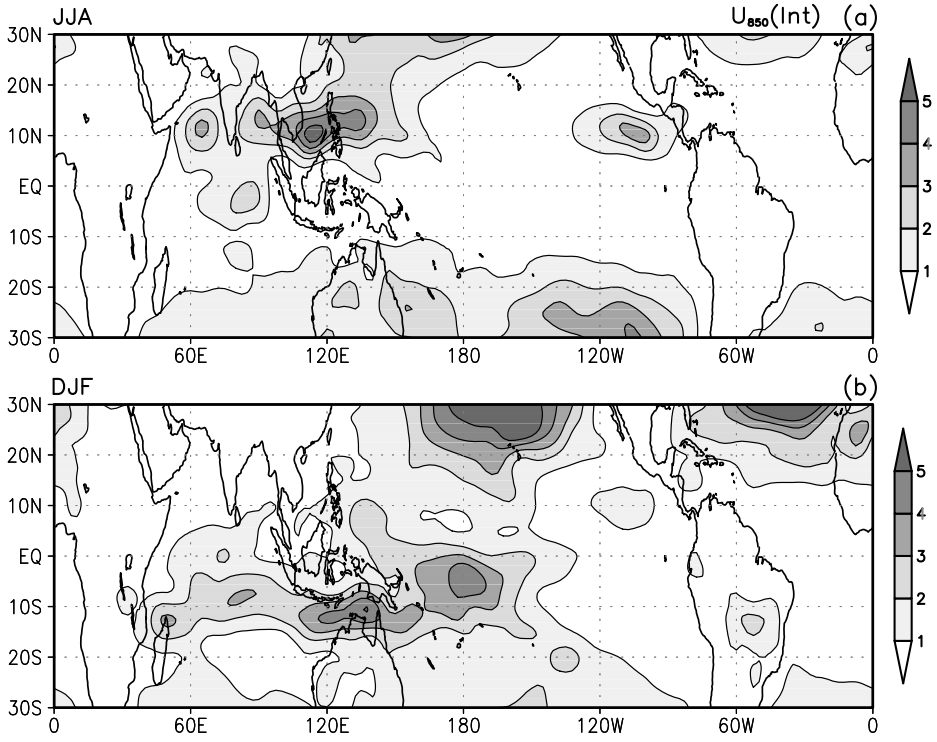

FIG. 7. The 'internal' variance of zonal winds at 850hPa (m^2s^{-2}) during (a) NH summer months (JJA) and (b) NH winter months (DJF).

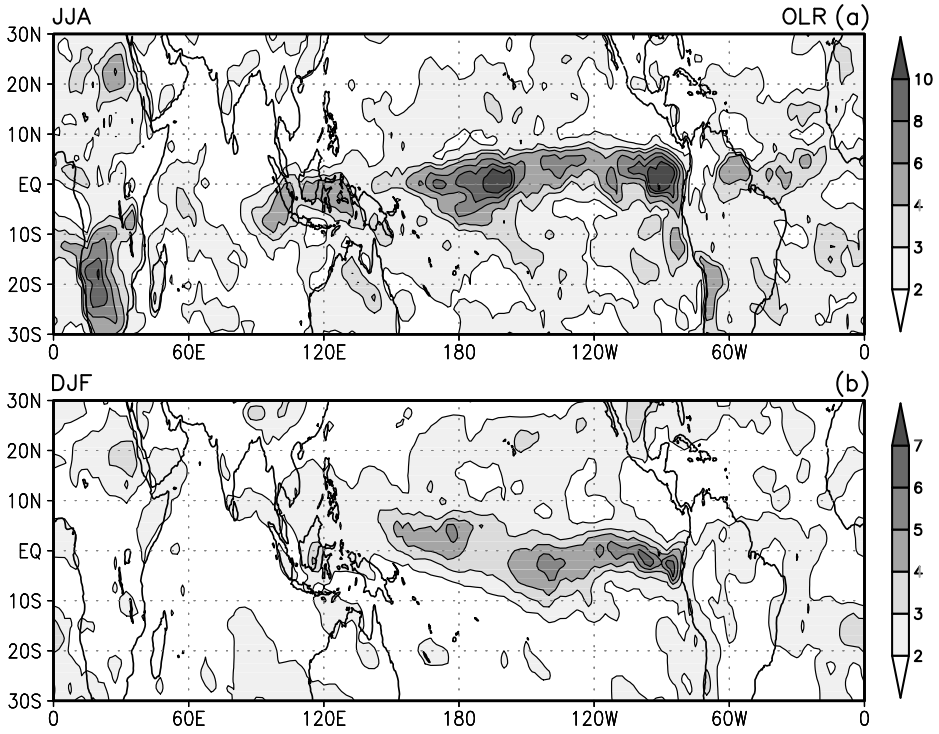

FIG. 8. Estimates of 'F' ratios for OLR (a) for all NH summer months (JJA) and (b) for all NH winter months (DJF) during the period 1980-1997.

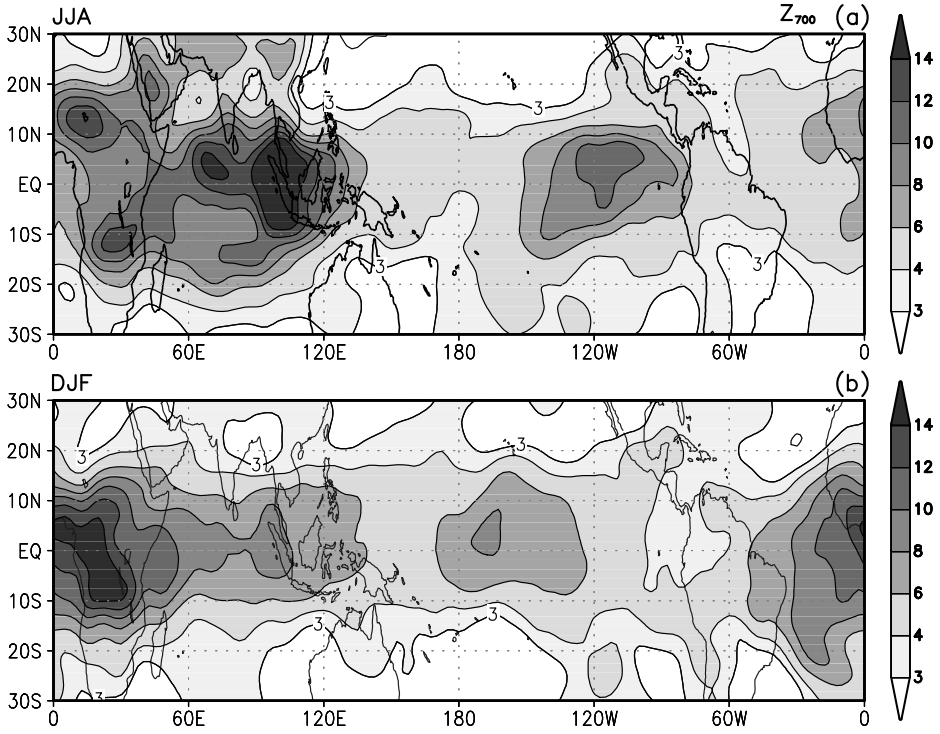

FIG. 9. Estimates of 'F' ratios for geopotential height at 700 hPa (a) for all NH summer months (JJA) and (b) for all NH winter months (DJF) during the period 1965-1997.

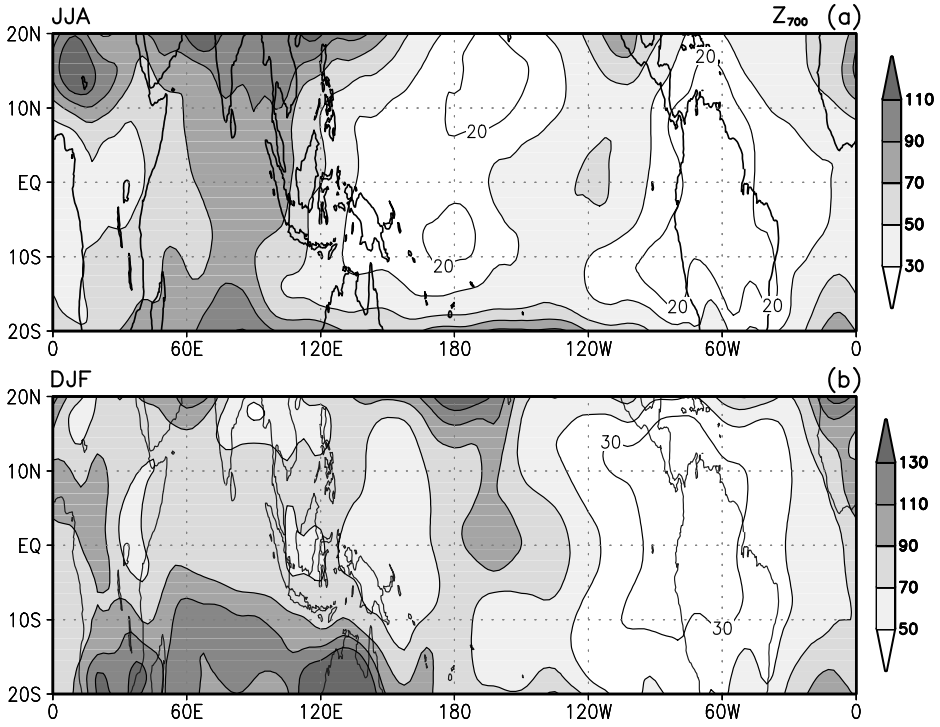

FIG. 10. The 'external' variance of geopotential height at 700 hPa (gpm^2) during (a) NH summer months (JJA) and (b) NH winter months (DJF).

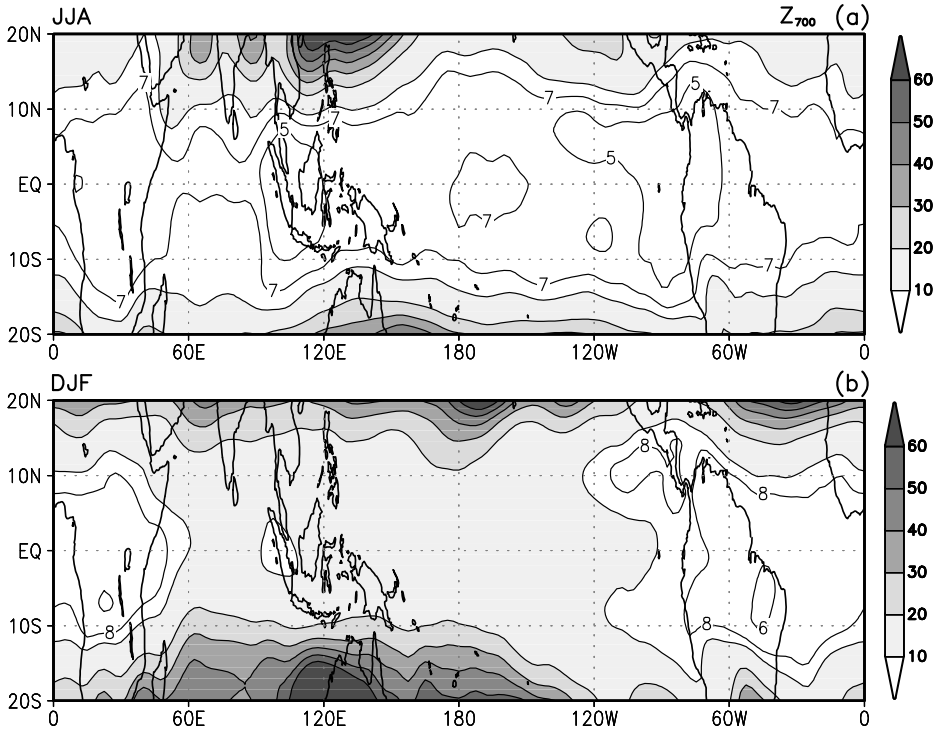

FIG. 11. The 'internal' variance of geopotential height at 700 hPa (gpm^2) during (a) NH summer months (JJA) and (b) NH winter months (DJF).

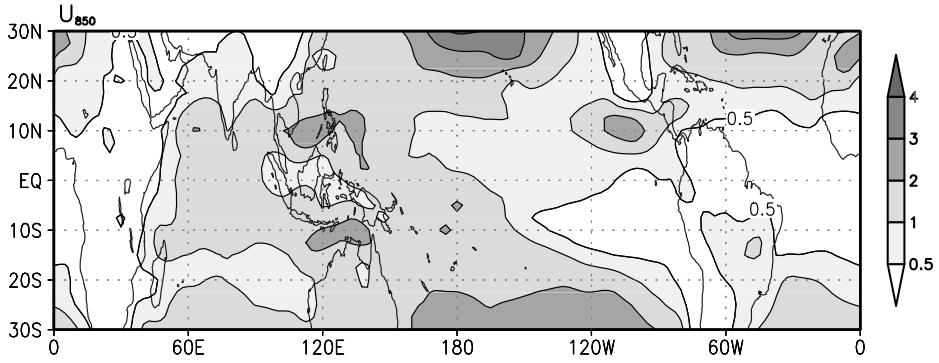

FIG. 12. The 'internal' variance of zonal winds at 850hPa (m^2s^{-2}) based on 396 months for the period January 1965 to December 1997 after removing the higher frequencies with period shorter than 10 days.

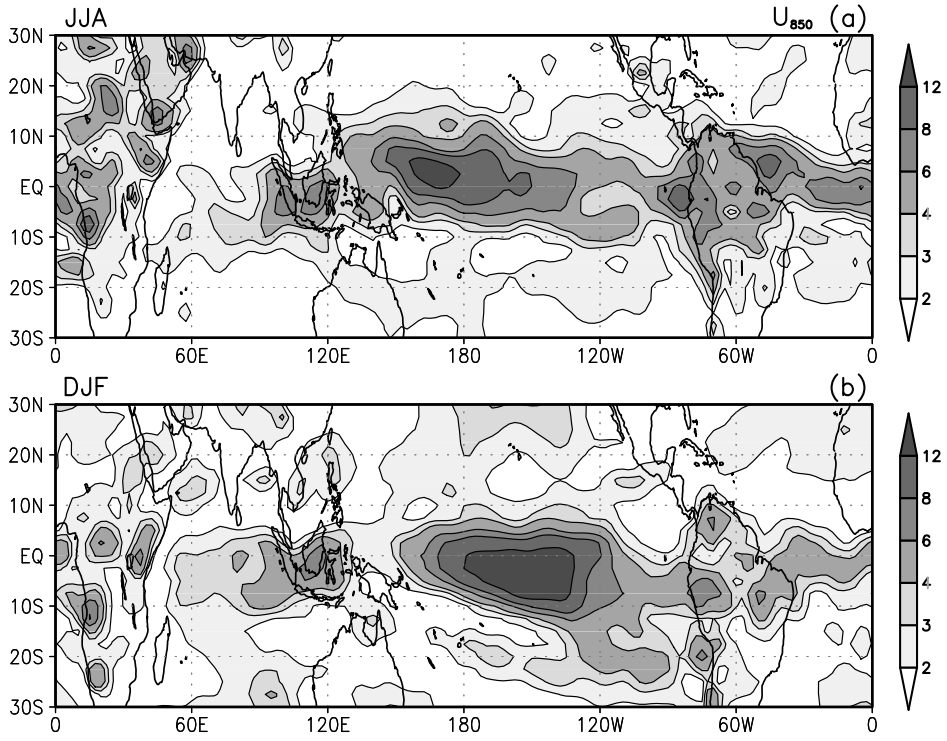

FIG. 13. Estimates of 'F' ratios for zonal winds at 850hPa for (a) NH summer season (JJA) (b) NH winter season (DJF).

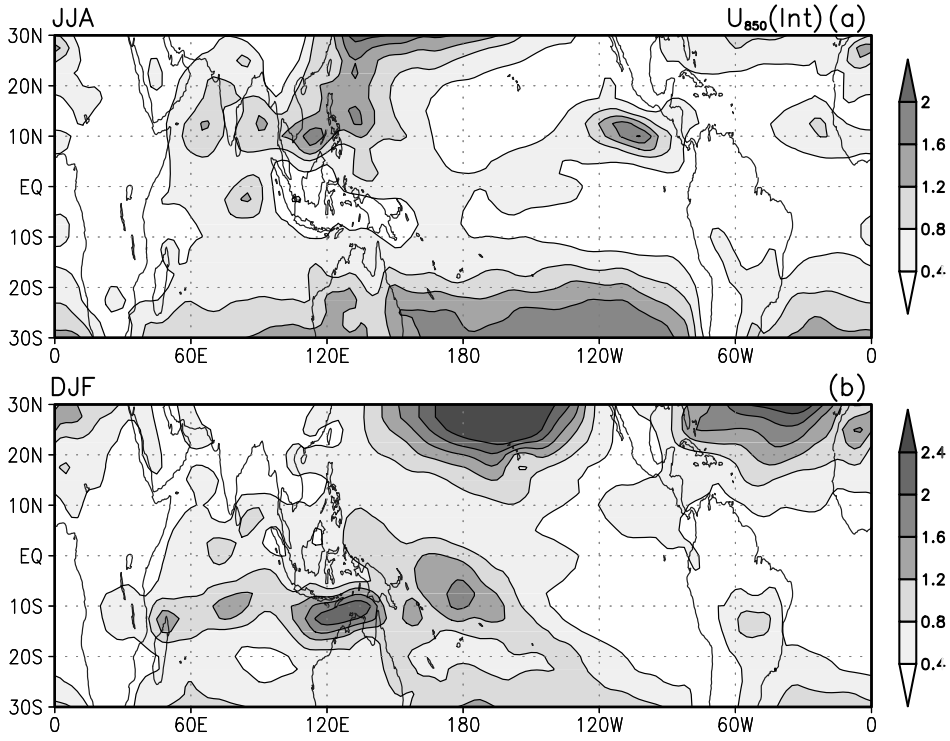

FIG. 14. Estimates of 'climate noise' for zonal winds at 850hPa for (a) NH summer season (JJA) (b) NH winter season (DJF).

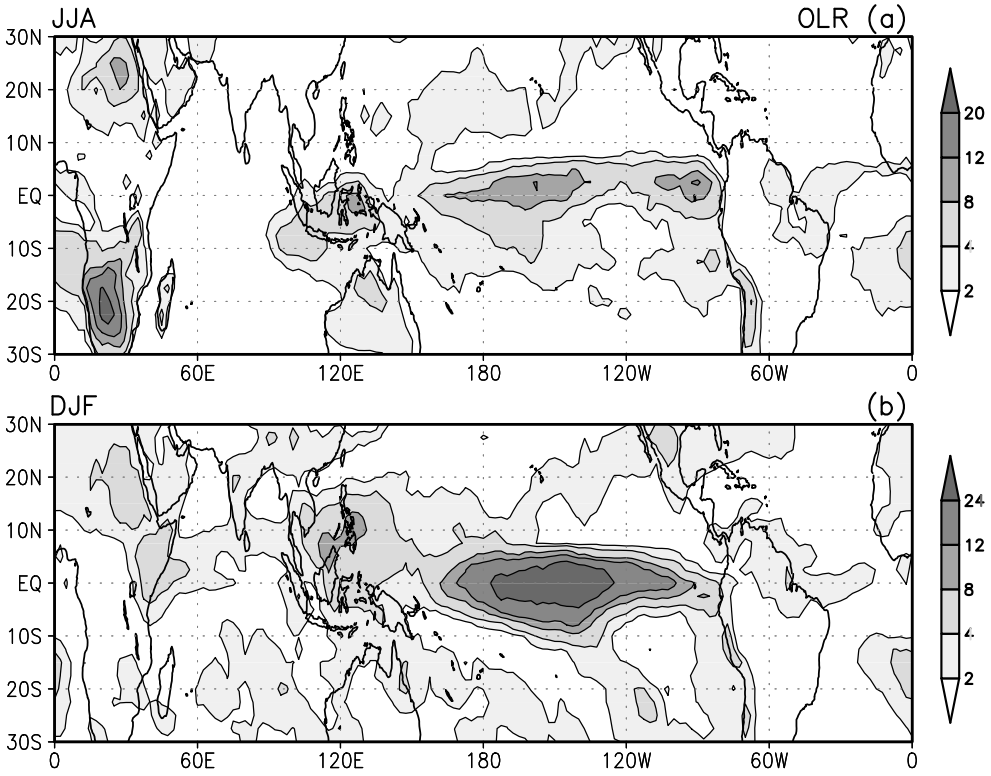

FIG. 15. Estimates of 'F' ratios for OLR for (a) NH summer season (JJA) (b) NH winter season (DJF).

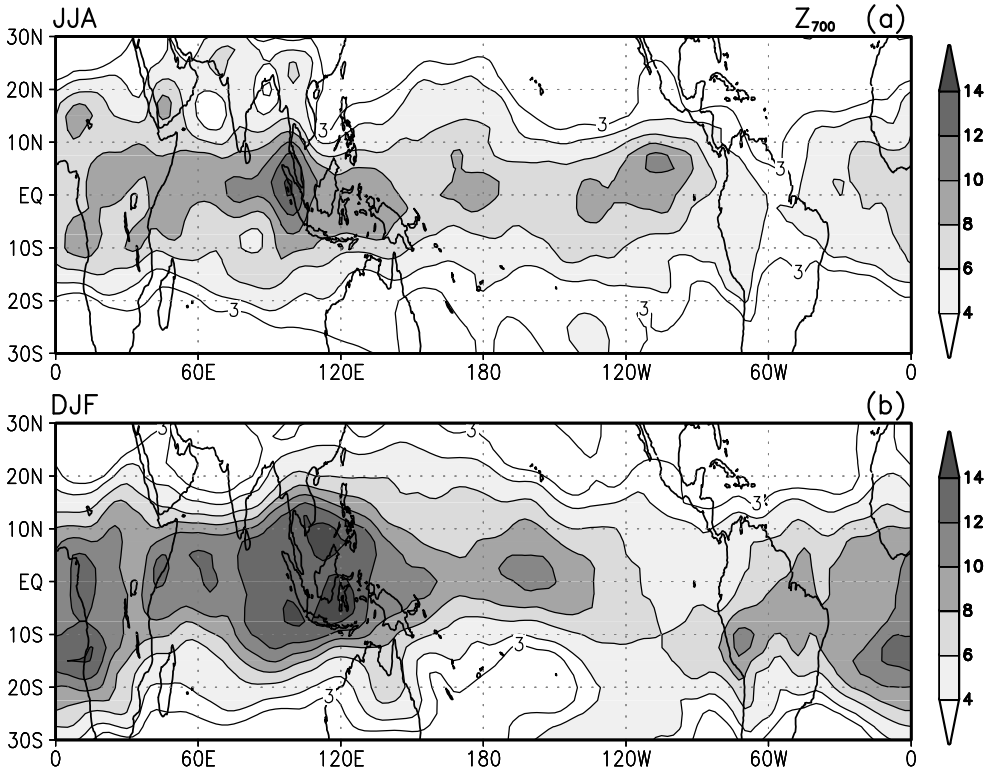

FIG. 16. Estimates of 'F' ratios for geopotential height at 700hPa for (a) NH summer season (JJA) (b) NH winter season (DJF).